Proceedings of The National Conference
On Undergraduate Research (NCUR) 2020
Montana State University, Bozeman MT
March 26-28, 2020

Designing a 2-μm Optical Parametric Oscillator for Enhanced Conversion Efficiency

Grant Levasseur
Electrical Engineering and Computer Science
United States Military Academy
606 Thayer Road
West Point, NY 10996

Faculty Advisor: Kirk Ingold

Abstract

Optical parametric oscillators (OPO) have gained wide use as both CW and pulsed optical sources throughout the past five decades. Following the first demonstration of a pulsed OPO in 1965, the invention of the modelocked laser in 1966 opened the field of OPOs to the regime of synchronously pumped OPOs. Synchronously pumped optical parametric oscillators (OPO) have become a primary tool for producing broadly tunable optical sources capable of generating picosecond and femtosecond pulses from the visible to mid-IR range. Most recently OPOs have been used to generate frequency combs; at degeneracy, or the half-harmonic, the OPO frequency and phase are intrinsically locked to the pump laser's frequency and phase, making this an ideal method for generating broadband, stable frequency combs. This research investigates a methodical design approach for optimizing the output efficiency of a half-harmonic OPO designed to convert femtosecond laser pulses centered near 1μm to an 'eye-safer' wavelength near 2μm. After thoroughly characterizing the Class IV, infrared pump laser, a mode-matching lens system is designed to efficiently match the mode of the pump laser to the cavity mode of a bow-tie ring-resonator cavity. A 1-mm length of Periodically Poled Magnesium Oxide-doped Lithium Niobate (PPLN) is used as the gain medium. After parametric oscillation is achieved, a Wollaston prism was characterized as a potential output coupling.

Keywords: Lasers, Nonlinear Optics, Optical Parametric Oscillators

1. Introduction

Degenerate synchronously pumped optical parametric oscillators (OPOs) have become a primary tool for extending near infrared frequency combs to the mid infrared range. In degeneracy high energy photons are split into two identical lower energy photons. Energy is conserved such that the energy of the high energy photons is equal to the converted lower energy photons. Degenerate OPOs have been previously shown to offer low thresholds, broad instantaneous bandwidths, and high conversion efficiencies.[1-3] Here a methodical approach is used to construct a degenerate OPO using a commercially available mode-locked near-IR femtosecond laser. Previous output coupling optimizations have yielded conversion efficiencies of up to 63%.[4] The difficulty of achieving a high conversion efficiency at 2μm is that there are limited polarizing and dichroic optics available above 1550nm. Using a Wollaston prism as an output coupling method shows potential because of its broadband efficiency. A detailed system design and characterization of a potential output coupling using a Wollaston prism show potential of producing similar or higher conversion efficiencies.

2. Method

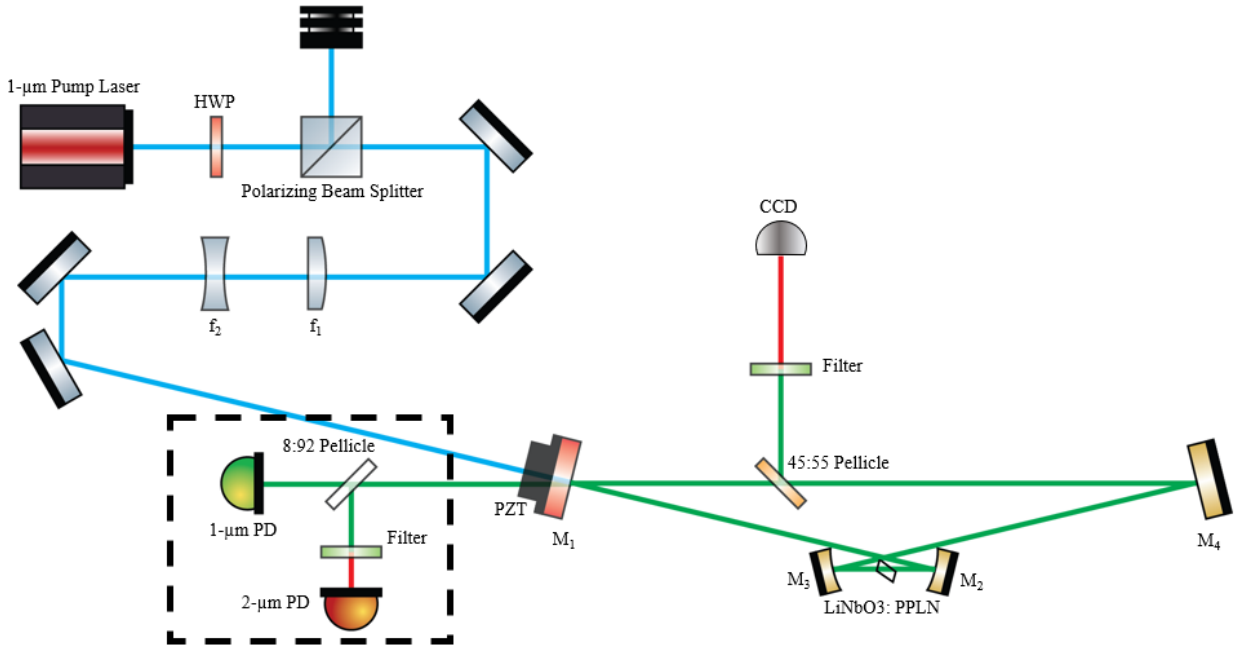

Figure 1. Schematic of the OPO setup. M_1 is a flat dichroic mirror with high transmission (> 96%) for the pump and high reflectivity from 1.7 - 2.3 mm (> 99%). Mirrors M_2 and M_3 are concave gold coated D-cut mirrors with a radius of curvature, R = 25.1 mm. M_4 is a flat gold coated mirror.

The pump laser for the OPO was a mode-locked Menlo Systems Orange A 1040-nm Ytterbium-doped fiber laser. This Class IV Laser provides approximately 99.3 fs pulses at an average power of 1W and a repetition rate of f_{rep}=250 MHz. The OPO setup is shown in Figure 1. A halfwave plate and polarizing beamsplitter cube are placed in the beam path to adjust the total power delivered to the OPO cavity. The polarizing beamsplitter cube transmits the P-polarization and reflects the S-polarization. A beam block is used to safely block the reflected beam. The half wave plate rotates the polarization of the pump thus adjusting the total amount of the laser power being transmitted to the cavity. A periscope (not shown) consisting of 2 low Group Dispersion Delay (GDD) ultrafast mirrors lowers the beam height to 2 inches above the optical table. The low GDD mirrors are used to minimize pulse spread as the beam traverses the optical setup.

The bowtie ring resonator is approximately 1.2m long to allow for successive round trips of the signal to overlap based on the repetition rate of the pump and the round-trip time of the cavity, according to , according to $\ell_{\text{cavity}} = c/f_{\text{rep}}$, where ℓ_{cavity} is the cavity length and c is the speed of light. Mirror M_1 is a dichroic mirror that is highly transmissive (T>99%) at 1µm and highly reflective at 2µm (R>99%). Mirrors M_2 and M_3 are 12.7-mm D-cut bare-gold coated mirrors with a radius of curvature of 25 mm. Mirror M_4 is a flat gold coated mirror. A 1-mm long Brewster cut Periodically Poled Magnesium Oxide-doped Lithium Niobate (PPLN) crystal is positioned at the center of the short arm between M_2 and M_3.

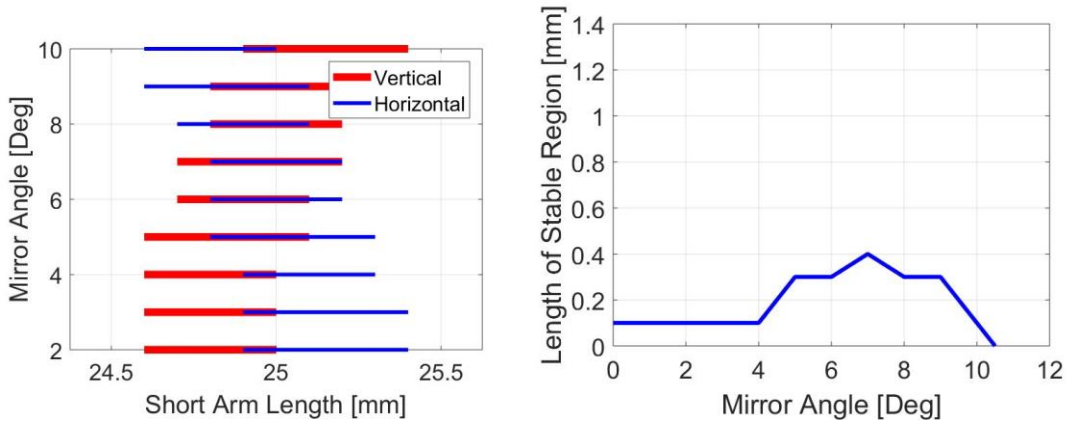

(a) (b)

Figure 2. OPO cavity calculated stability regions. (a) Plot of the stability lengths in both vertical and horizontal versus the mirror angle. (b) Length of stability region at each cavity mirror angle.

The Brewster-cut of the PPLN crystal combined with the tilt of the curved gold mirrors creates an astigmatism of the beam (between the vertical and horizontal dimensions) within the cavity.[5] Consequently, only certain mirror angles allow stable resonance at the pump wave. Cavity simulations shown in Figure 2(a) show the common short arm lengths (the length between M_2 and M_3) at which both the vertical and horizontal orientations are stable. The optimal angle of incidence of 7° produces a cavity stability length range of 400 µm as shown in Figure 2(b). Using the optimal angle of incidence and length of the bowtie resonator, the dimensions of the cavity were calculated. The short arm length was set to 25.1mm which is close to the focal length of M_2 and M_3 and falls roughly within the center of the stability range of the cavity.

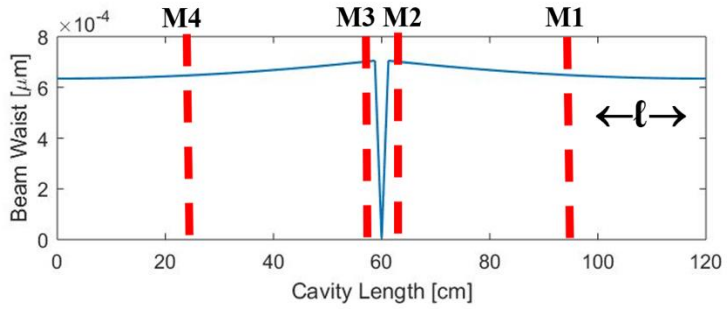

Figure 3. Beam waist as it traverses the cavity. The beam waist from the midpoint between M_1 and M_4 to M_1 is labelled ℓ and must match the pump beam entering the cavity.

Figure 3 shows the beam calculated beam radius as it traverses the cavity. Within the resonator, there are 2 minimum beam waists, one in the center of the short arm between M_3 and M_2, and one in the center or the long arm between M_4 and M_1. The PPLN crystal is placed at the beam waist in the short arm at the point of beam waist to maximize the gain in the system. For successful modematching to occur, the pump beam waist must match the calculated beam waist above in Figure 3.

To maximize conversion efficiency, the gain coefficient through the PPLN must be maximized. The gain coefficient, and subsequent conversion efficiency of a phase-matched system in the PPLN is given by Equation 1,

$$\Gamma^2 {l_{PPLN}}^2 = \frac{2\omega^2 |d_{eff}|^2 {l_{PPLN}}^2 I(\omega)}{n^3 c^3 \varepsilon_0} \quad (1)$$

where Γ is the gain coefficient, I is optical intensity of the fundamental wavelength, ω is the angular frequency, d_{eff} is the effective coefficient of second-order nonlinearity, n is the refractive index. Many variables in Equation 1 are constants such as the speed of light, c, and the permittivity of free space, ε_0. Minimizing the beam size in the PPLN, maximizes the intensity, as intensity is inversely related to the beam size. The gain coefficient, Γ, is therefore, a function of intensity, I. The intensity of the pump can be maximized by minimizing the beam size at the beam waist and that the beam waist is in the center of the PPLN. The beam waist at the PPLN is adjusted by adjusting the short arm length within the stability region.

Length ℓ is the distance from Mirror 1 back to the center of the long arm of the cavity. The characteristics of the beam at this length must be mimicked on the input side of the dichroic M_1. To achieve optimal modematching, the pump laser was first characterized using a CDD Camera Beam Profiler (BC106N-UV) and M^2 Measurement System. The calculated M^2 of the system was 1.11. By using the characterization of the pump laser and what the beam must look like as it enters the cavity, a lens system can be designed to fit the necessary beam geometry. Ray transfer matrices were used to determine the necessary lens required to match. This is accomplished through the lens system of f_1 and f_2. The lenses used were made of UV Fused Silica (UVFS). UVFS was used over traditional BK-7 glass because it has a slightly lower group velocity dispersion and testing showed that it had approximately the same transmittivity.

Once the pump laser was matched to the cavity. The total cavity length was altered by adjusting the linear stages on which the M_1 and M_4 were mounted. Using a CCD camera, the reflection of the incoming pump pulse and leakage through the dichroic mirror after the first-round trip were captured. The cavity was adjusted so that both pulses were spatially overlapped on the camera. As adjustments became finer, the second-round trip became visible and overlapped spatial with the initial reflection and first round trip.

An IR photodetector connected to an oscilloscope replaced the CCD camera and monitored the temporal overlap of the pump and the successive roundtrips pulses. A piezo crystal attached to the stage with M_1 swept the cavity length by several micrometers at 10Hz. The cavity length was adjusted using the translation stages until the pump reflection and cavity leakage created an interference pattern shown in Figure 4. The interference indicates that the pump pulses were temporally overlapping.

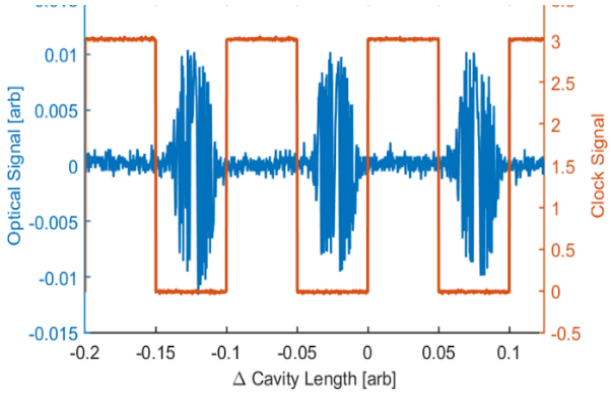

Figure 4. Oscillation of the pump caused by successive roundtrips overlapping as the PZT dithers the cavity length.

While interference indicates near resonance, it is not frequency conversion. This is achieved by further adjusting the cavity length and piezo stage. This is done through an iterative process of optimizing the roundtrip beam overlap using the CCD camera and the cavity length using the 1-µm photodetector. Given 1-µm photodetector and the CCD camera are silicon-based detectors, they are unable to detect 2-µm. During this iterative process, it is assumed that the 2-µm signal and 1- µm signal occupy the same space. The 1-µm signal is depleted as it is converted to 2-µm. An 8:92 pellicle beamsplitter was placed before the IR photodetector reflection a portion of the signal 90° to a PbSe detector. The band gap of PbSe is capable of detecting the 2-µm signal. As the piezo stage dithers the cavity length, the 1-µm depletion can be seen at discrete intervals by the photodetector. Using the half-wave plate to adjust the pump power, threshold was measured by reducing the pump power until the pump depletion and generated 2-µm signal disappear.

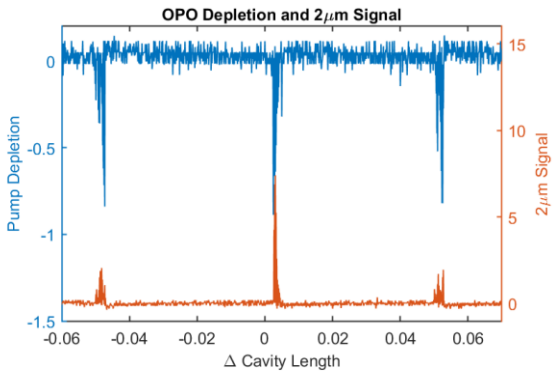

Figure 5. Depletion of the 1-µm pump as it is converted to the 2-µm signal at discrete resonances along the length of travel of the PZT

Continuous operation of the OPO is achieved through the locking of the cavity length to one of the discrete cavity lengths that where the 2-µm signal is generated. This cavity length was maintained through an electronic PID locking circuit. The feedback loop controller is attached to the pump, 2-µm photodetector, and the piezo actuator on M_1. The circuit locks the cavity length in sync with the pump repetition rate keeping the 2-µm signal at the peak of one of the resonance lengths.

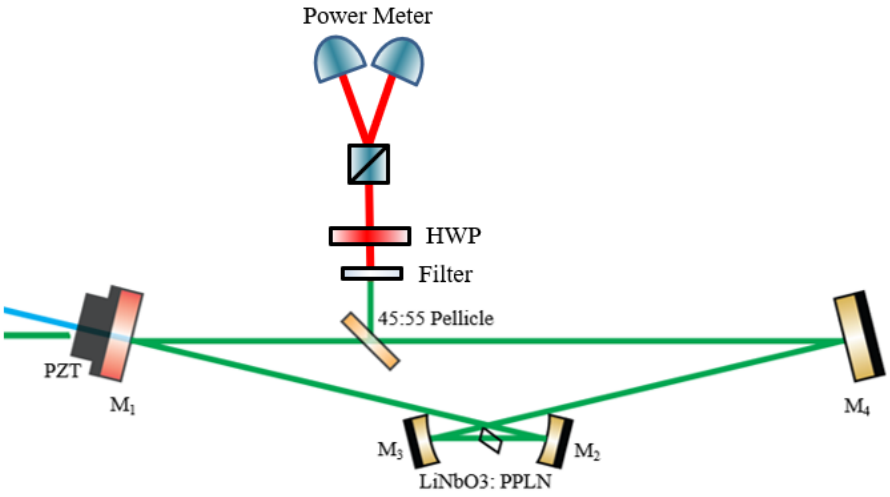

Figure 6. Schematic of the characterization of the Wollaston Prism by measuring the relative power of both the parallel and perpendicular outputs of the prism as the half wave plate is rotated.

A WPM10 Magnesium Fluoride Wollaston prism beamsplitter and HWP were characterized as a possible output coupling method as shown in Figure 6. This specific beamsplitter has a deviation angle of 1°20’ for both outputs. While a Rochon prism would make outcoupling easier as one of the outputs would not be deviated, the Wollaston prism chosen had the lowest dispersion and highest transmission. A 45:55 pellicle beamsplitter placed in the long arm of the cavity outcoupled a portion of the beam. Using a long-pass filter with a cutoff of 1.8µm to separate the pump and signal beams, this beam was passed through the half wave plate to the Wollaston prism. Because the beam is already perpendicularly polarized, rotating the halfwave plate controls the proportion of the power being divided amongst the perpendicular and parallel outputs.

3. Results

The lowest achieved pump threshold for the OPO was 50mW for the 1-mm PPLN. This was before an output coupler was placed in the cavity. 50mW of average pump power corresponds to a pulse energy of roughly 200pJ and a peak power of 2kW. This can be compared the 1W average power of the unreduced pump laser, which corresponds to a peak power of 40kW. The threshold for frequency conversion is low compared to the full pump power showing that the total loss of the system is low.

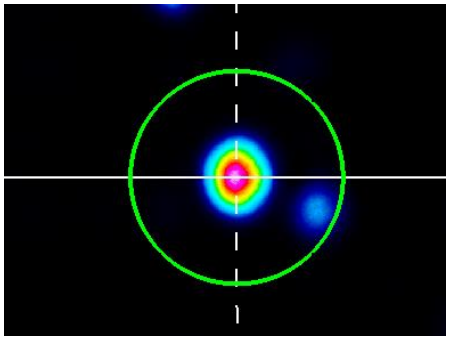

Figure 7. CCD capture of the 2-µm beam using a 45:55 pellicle beamsplitter to outcouple it from the OPO cavity.

To initially outcouple the beam, a 45:55 pellicle beamsplitter was place in the long arm of the cavity. Passing the outcoupled beam through the long pass filter to an IR CCD camera allowed us to capture 2-µm shown in Figure 7. The image shows that the beam is slightly elliptical with a measured ellipticity of 87.6%. While there is still distortion of the beam, it is still mostly gaussian. The additional nodes around the beam are artifacts from reflections from the Germanium neutral density filters placed on the CCD camera.

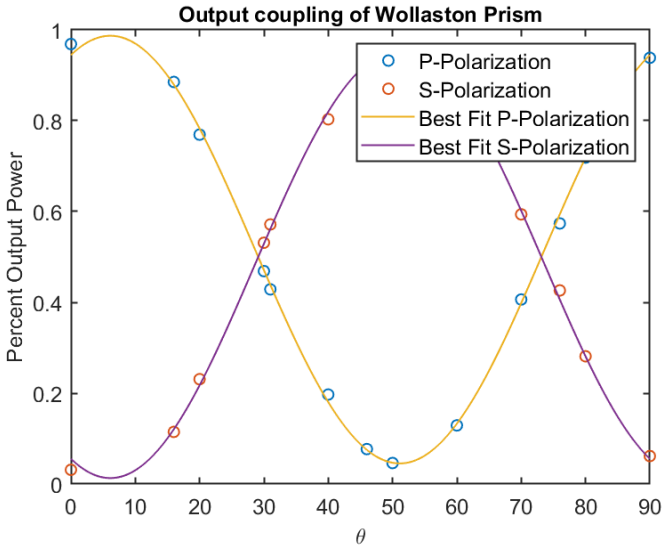

S-Polarization:

$y = 0.94 * \sin(2\theta - 12.25)^2 + 0.01$

P-Polarization:

$y = 0.94 * \cos(2\theta - 12.25)^2 + 0.045$

Figure 8. Relative power output measurements of each polarization as a function of half wave plate rotation and their best fit line.

The characterization of the 2-µm beam through the Wollaston Prism is shown in Figure As the half wave plate is rotated, the resulting output is shifted from the P-Polarization to the S-polarization. The Best-Fit Lines plotted along the measured points show the predictability and wide range of relative output powers possible. The outcoupling threshold of the lies within the measured range of the prism. The equations also show that with this specific half wave

plate mounted is slightly rotated in its holder. The half wave plate is rotated 6.12° in its holder. It has shown to be a viable possibility for providing a variable output coupling.

4. Conclusion and Future Work

A synchronously pumped degenerate OPO was successfully designed and implemented. A variable outcoupling method using a Wollaston prism was also characterized for future implementation. Future work would include implementing the outcoupling method into the cavity and determining the outcoupling threshold of the OPO. Because the Wollaston prism deviates both outputs, the cavity would need to be readjusted to compensate. A characterization of the output would include spectrum analysis using an Optical Spectrum Analyzer and pulse length using Frequency-Resolved Optical Gating (FROG). A Rochon prism could be characterized in the same method as the Wollaston prism and compared. The use of a Rochon prism would require less adjustments to outcouple, but the results would be less accurate. Based on the outcoupling results, M_4 would be replaced with a dielectric mirror matching this threshold to achieve maximum conversion efficiency while limiting dispersion. By applying the Wollaston prism as the variable outcoupling method an accurate measurement of the necessary dielectric mirror can be determined.

5. References

1. Leindecker, Nick, Alireza Marandi, Robert L. Byer, and Konstantin L. Vodopyanov. “Broadband Degenerate OPO for Mid-Infrared Frequency Comb Generation.” *Optics Express* 19, no. 7 (March 28, 2011): 6296.
2. Leindecker, Nick, Alireza Marandi, Robert L. Byer, Konstantin L. Vodopyanov, Jie Jiang, Ingmar Hartl, Martin Fermann, and Peter G. Schunemann. “Octave-Spanning Ultrafast OPO with 26-61μm Instantaneous Bandwidth Pumped by Femtosecond Tm-Fiber Laser.” *Optics Express* 20, no. 7 (March 26, 2012): 7046.
3. Rudy, Charles W., Alireza Marandi, Kirk A. Ingold, Stephen J. Wolf, Konstantin L. Vodopyanov, Robert L. Byer, Lihmei Yang, Peng Wan, and Jian Liu. “Sub-50 Fs Pulses around 2070 Nm from a Synchronously-Pumped, Degenerate OPO.” *Optics Express* 20, no. 25 (December 3, 2012): 27589.
4. Ingold, Kirk A., Alireza Marandi, Charles W. Rudy, and Robert L. Byer. “2.09-Mm Degenerate Femtosecond OPO with over 60% Conversion Efficiency and 0.6-W Output.” In *CLEO: 2014*, SM2I.4. San Jose, California: OSA, 2014.
5. H. Kogelnik, E. Ippen, A. Dienes and C. Shank, "Astigmatically compensated cavities for CW dye lasers," in IEEE Journal of Quantum Electronics, vol. 8, no. 3, pp. 373-379, March 1972.